Aerodynamic behavior of the bridge of a capacitive RF MEMS switch

Dragos ISVORANU [1,*], Stefan Sorohan [2], Gabriela CIUPRINA [3]

* Corresponding author: Tel.: ++40 (0)213250704; Fax: ++40 (0) 213181007; Email: ddisvoranu@gmail.com
1 Elie Carafoli Dept. of Aerospace Sciences, University Politehnica of Bucharest (UPB), Romania (RO)
2 Department of Strength of Materials, Faculty of Engineering and Management of Technological Systems, UPB, RO
3 Department of Electrotechnics, Electrical Engineering Faculty, UPB, RO

Abstract The present paper proposes a coupled 3D multi-physics model and presents the results of its transient simulation, for a RF MEMS capacitive switch of bridge-type. The fluid structure interaction (FSI) simulation sustains time-varying viscous damping and modified time response of the bridge deflection compared to the actuation modulation above closing of the switch. Complex 3D geometries of the bridge were rarely taken into account in viscous damping assessment much less in the simulation of the full flow around the bridge of the switch. The final goal of the paper is to obtain the dependency of an equivalent damping coefficient with respect to time, to be used in subsequent reduced order models for the switch, that include the aerodynamic behaviour of the switch.

Keywords: Capacitive switch, Coupled FSI modelling, Vortex flows, Viscous damping

1. Introduction

An RF MEMS switch is an integrated device that uses a mechanical movement to change the configuration of a radio frequency (RF) circuit. It is a microelectromechanical system (MEMS), fabricated using the micromachining technology. In our case, the switch ensures a short-circuit or an open state of a transmission line through which a RF signal is allowed or not to pass. Capacitive switches, with their large contact area, can handle more RF power than metal-to-metal contact switches and are therefore the preferred switches for applications requiring 100–500 mW of RF power. Their switching time is in the range of 1-200 μs. Their relatively small contact forces (50-1000 μN) ensure high reliability and a large number of operating cycles (~ 2-10 Billions). Capacitive switches can operate in the range 6 – 120 GHz and above due to their relatively small down-state capacitance (2–5 pF). Among all these parameters, the switching time is an important one, especially in applications in which the devices are required to change their states as fast as possible. Therefore, modelling strategies able to accurately predict the switching time of RF MEMS switches are needed.

There is an enormous literature on the modelling steps in the case of static regimes, useful to derive quantities such as the pull-in or pull-out voltages, based on the coupling between the mechanical and the electrostatic field formulations. However, in the dynamic case, neglecting or poor models of the aerodynamic behaviour may lead to unsatisfactory results (Errikson, 2005). Most papers dealing with aerodynamic behaviour use the squeeze film analysis mainly related to viscous damping characteristics (Steeneken et al., 2005). Complex 3D geometries of the bridge were rarely taken into account, with few exceptions (Mohite et al. 2008), in viscous damping assessment much less in the simulation of the full flow around the bridge of the switch. That is why, the present paper includes, beside the common assessment of the pull-in, bridge deflection, capacitance and mechanical behaviour a 3D fluid order to catch the complex vortical unsteady fluid structures

that have been identified in our preliminary finite element analysis tests.

The most important design goals for dynamic MEMS devices such as accelerometers, microphones, tuning-fork gyroscopes, micro-switches, micro-mirrors, etc., are high sensitivity and high resolution.

At the design level of MEMS parallel-plate capacitive transducers for these applications, maximizing the mechanical compliance (depending on the ratio between the area and the thickness of the plate) and the base capacitance (depending on the ratio between area and air-gap) of the structures are the means by which one can fulfil the aforementioned goals. This clearly requires sufficiently high surface area and small thickness of the vibrating structure, as well as a very small air-gap separating the two structures. However, the air in the small gap between the transversely moving planar structure and the fixed substrate induces damping, rigidity, and inertial forces to the structures (Andrews, 1993, Veijola, 2001-2004). These forces have a complex dependence on the air-gap height and the operating frequency. These forces affect the frequency response of the structure and, hence, the sensitivity, resolution, and bandwidth of the device. Damping due to the squeeze-film is considerably high for large surface-to-air-gap ratio. At low frequencies, damping dominates, whereas at high frequencies, inertial effects dominate. Damping can be minimized if it is possible to operate the device under a vacuum condition, which, in turn, requires expensive packaging. The amount of squeeze-film damping can be controlled by providing perforations in either the back plate or the oscillating proof mass. These perforations also facilitate the etch release of the sacrificial layer in surface micromachining but reduce the device capacitance, which is undesirable. An adequate value of the base capacitance can be obtained by reducing the air-gap. While reducing the gap, the perforations need to be designed such that constant damping is maintained without sacrificing the capacitance. A feasible range of perforation geometry depends on the chosen micromachining process. To achieve the design goals of minimizing damping and maximizing the capacitance, a trade-off analysis must be carried out between the perforation geometry and the air-gap.

2. Physical modelling

The mathematical-physical model describing the RF-MEMS switch movement comprises the flexible beam deformation equations, the electrostatic force assessment and the Navier-Stokes equations which model the air flow around the bridge. The system is nonlinear due to the nonlinear nature of the squeeze-film force, nonlinear rigidity of mid-plane stretching, and the nonlinear electrostatic force. Assuming that we have no structural damping, the coupled system of equations reads

$$\mathbf{M}\ddot{\mathbf{u}} + \mathbf{K}\mathbf{u} = \mathbf{F}^{(el)} + \mathbf{F}^{(p)} \tag{1}$$

$$\rho\frac{\partial \mathbf{v}}{\partial t} + \rho\mathbf{v}\cdot\nabla\mathbf{v} = -\nabla p - \nabla\cdot\mathbf{\Pi} \tag{2}$$

where $\mathbf{u}$ is the displacement vector, $\mathbf{M}$ structural mass matrix, $\mathbf{K}$ the structural stiffness matrix, $\mathbf{\Pi}$ is the stress tensor and $\mathbf{v}$ the velocity vector. Pressure p and density ρ are the other quantities present in Eq. 2. The software ANSYS proposes different solutions (including strong and weak formulations) to achieve the equilibrium between electrostatic forces and mechanical structure. One possibility is to use the TRANS126 element (Gyimesi and Ostergaard, 1999). It is a strong coupled transducer formed by two node lines. The gap between the plates is discretised by one-dimensional condensers (micro-condensers) that connect nodes on structure with nodes on the substrate. The variables are the voltage V and the displacement. The electric force in a micro-condenser is then computed as

$$F^{(el)} = \frac{1}{2}\frac{dC}{dh}V^2 \tag{3}$$

where C is the capacitance of the micro-condenser, also depending on the gap h between the plates (Avdeev, 2003).

The aerodynamic force $F^{(p)}$ is the result of the pressure distribution over the bridge and is the quantity that couples the electro-

mechanical system and the fluid system.

A model of the RF MEMS switch is represented in Fig. 1. The major dimensions of the bridge are 910x200x2 μm (length, width and thickness). The gap size is 2.5 μm.

The aerodynamic behaviour of the bridge can be expressed mainly in terms of aerodynamic forces. In the present case the most important force is the drag force acting on the moving structure.

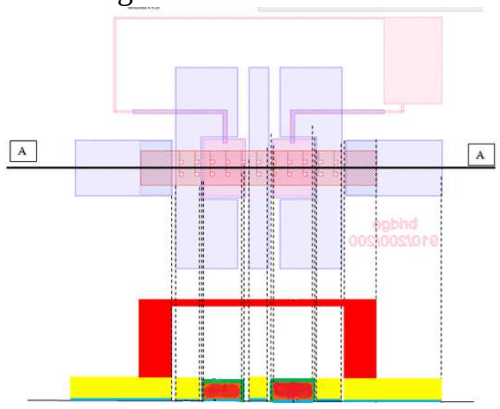

Fig. 1. Bridge layout. The dimensions of A-A section are not to scale.

The aerodynamic behaviour of the bridge can be expressed mainly in terms of aerodynamic forces. In the present case the most important force is the drag force acting on the moving structure. The most common way of assessing the drag force is by using Reynolds equations, either incompressible or compressible. In this case, because of the small velocities implied, the damping coefficient can be evaluated as

$$c = -\frac{F^{(p)}}{dh/dt} \tag{4}$$

where h is the instantaneous gap size. Linearization of the Reynolds equations for small pressure and small displacement compared with the reference pressure and gap size, leads to a viscous damping coefficient dependence on the excitation frequency. For the rigid plate of length L and width w, the lower limit is (Bao, 2007):

$$c = \mu L\left(\frac{w}{h_0}\right)^3\left(1-0.58\frac{w}{L}\right),\ \omega \to 0 \tag{5}$$

where ω is the circular frequency, h_0 is the initial gap and μ the molecular viscosity. The same conclusion is sustained also by other theoretical studies (Lee, 2011, Steeneken et al., 2005). The only difference is related to the expression in the second bracket in Eq. (5). It seems that, apart from a possible dependence on time through viscosity, this coefficient is constant (Jazar, 2012). Because the air-gap is a rarefied domain, it follows that time variation of the damping coefficient is a result of relation between Knudsen number and effective viscosity, like for example (Veijola, 1999):

$$\mu_{eff}(t) = \frac{\mu}{1+9.638[Kn(t)]^{1.159}} \tag{6}$$

where

$$Kn(t) = Kn_{ref}\frac{p_{ref}}{p(t)}\sqrt{\frac{T(t)}{T_{ref}}}\frac{h_0}{h_0+h(t)} \tag{7}$$

Other studies indicate a strong dependence of the damping coefficient with the frequency of the actuation (Mohite et al., 2008). For much of the frequency range this dependence is linear.

The goal of our paper is to assess a more realistic time dependence of the damping coefficient to be used later on in reduced order model that includes not only the structural and electric behaviour of the switch but also the viscous damping phenomenon.

3. Numerical approach

The electrostatic capacitive RF MEMS bridge is an example of coupled field analysis where the input of one field analysis depends on the results from another analysis. In the present case this dependence involves a two-way coupling. The ANSYS Multi-field solver, available for a large class of coupled analysis problems, is an automated tool for solving load transfer coupled field problems. The solver uses iterative coupling where each physics is solved either simultaneously or sequentially, and each matrix equation is solved separately. The solver iterates between each physics field until loads transferred across the physics interfaces converge. Within each time step there is the stagger loop. The stagger loop allows for implicit coupling of the fields. Strongly coupled fields should be solved sequentially which ensures that the most recent

results/loads from one field solver are applied to the other.

Our approach consists of coupling the Ansys transient structural analysis with CFX fluid solver. Taking advantage of the symmetry, the full model was cut in half. The fluid domain was split in two sub-domains, one beneath the bridge and the rest surrounding the solid structure and filling in the box shape depicted in Fig. 2. The advantage of this approach is related to using different fluid properties (e.g. viscosity) in either fluid sub-domain. Fluid in both fluid domains is at constant 288 K temperature. The reference pressure is 101325 Pa. The exterior fluid domain has constant transport properties, in particular $\mu = 18.2 \cdot 10^{-6}$ Pa·s, while within the inner (beneath the bridge) fluid domain, viscosity depends on the local Knudsen number as in Eq. (6). Another advantage of the split fluid approach comes from the fact that the inner fluid domain can be discretized very easily with prisms, thus avoiding the folding of the moving mesh.

Symmetry boundary conditions, both for the mechanical analysis and for the fluid analysis, were imposed in the symmetry plane. No slip boundary conditions were considered for the bottom wall. Opening conditions were imposed on all lateral walls as well as the top wall.

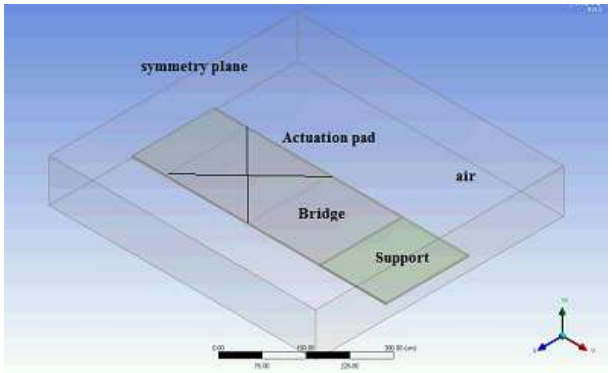

Fig. 2. 3D half model of the bridge.

The material of the bridge is gold with Young modulus of 78 GPa and Poisson ratio of 0.44. The bridge structural grid has 8000 elements out of 15700 elements for the whole structure (bridge plus supporting pad). The fluid domain was discretized with 473000 elements.

4. Results

The first step in our endeavour is performing a steady structural analysis in order to evaluate the pull-in voltage. Related to this step, a grid independence test was pursued in order determine the best structural grid size for future transient analysis. The results are presented in Fig. 3.

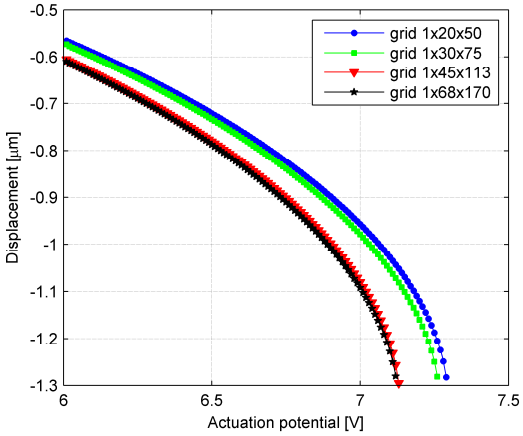

Fig. 3. Grid independence test

The conclusion of the test is that the third grid (1x45x113) can be successfully used for future analysis and the static pull-in voltage is $V_{pi} = 7.13\,\mathrm{V}$.

Next, a modal analysis revealed that the natural frequency of the bridge is around 5200 Hz.

For the transient analysis two cases were taken into account: a Dirac-type load for 1 µs (Fig. 4) and a step load of different duration (Fig. 5). In both cases, the transient structural analysis yielded the maximum amplitude (or duration) of the load that ensured passing beyond the mechanical instability that leads to air gap closing. The idea of loading with a Dirac-type load is related to the assessment of the viscous damping when other modes beside the fundamental one are excited. The Dirac load was performed with various amplitudes, resulting that a 70 V load yields the closing of the switch. In the case of the step load with various durations, a step load of 95 µs will drive the switch in the closed position. These assessments were made taking into account the maximum displacement of the bridge which

happens for a point in the area of the actuation pad.

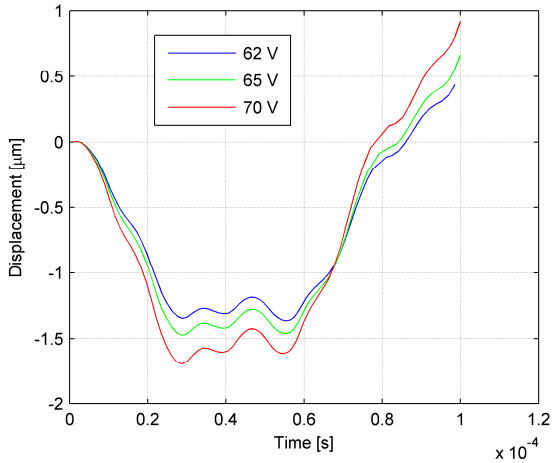

Fig. 4. Response of the bridge for Dirac-type load for the midpoint in the symmetry plane.

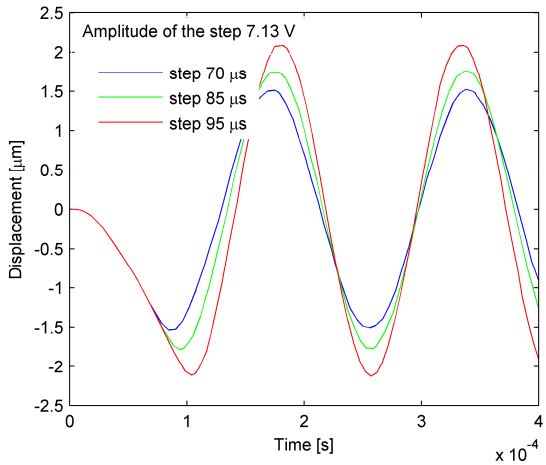

Fig. 5. Response of the bridge for step load for the midpoint in the symmetry plane.

The results of the coupled structural-electrostatic-fluid analysis are presented below for the 62 V Dirac case and 70 μs step case. These choices are justified by the non-closed switch position condition hypothesis.

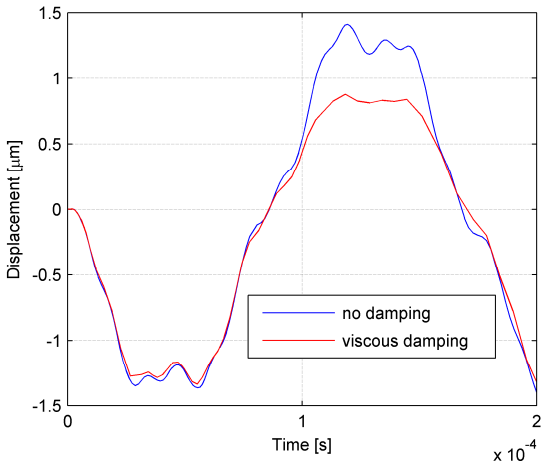

Fig. 6. Dirac-load response with and without viscous damping (same point like in Figs. 4-5).

The viscous response of the bridge smoothes the higher modes especially on the opening phase of movement but does not affects the natural frequency of the oscillation.

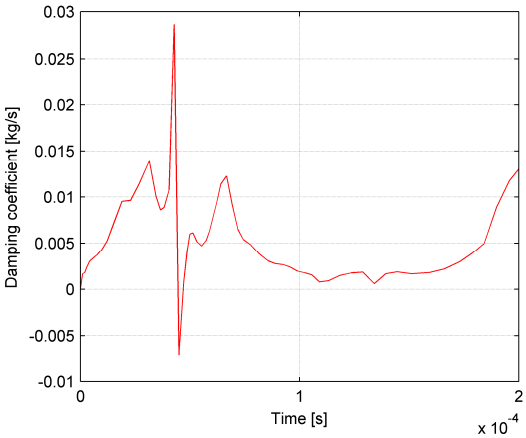

Fig. 7. Time variation of the damping coefficient.

The most intriguing feature resulting from Fig. 7 is that the average velocity of the bridge and the aerodynamic force are not in phase and there is a certain phase delay between them that yields the damping coefficient negative.

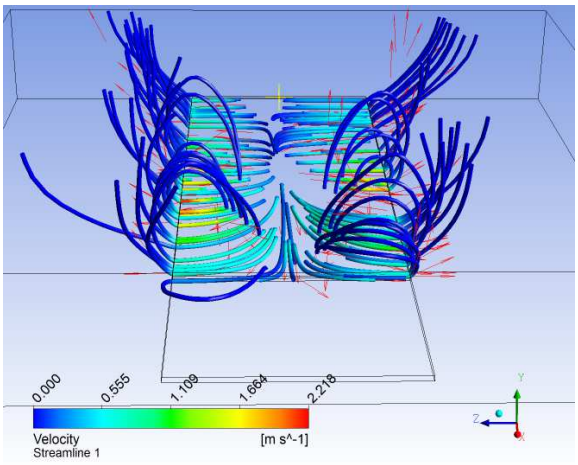

a)

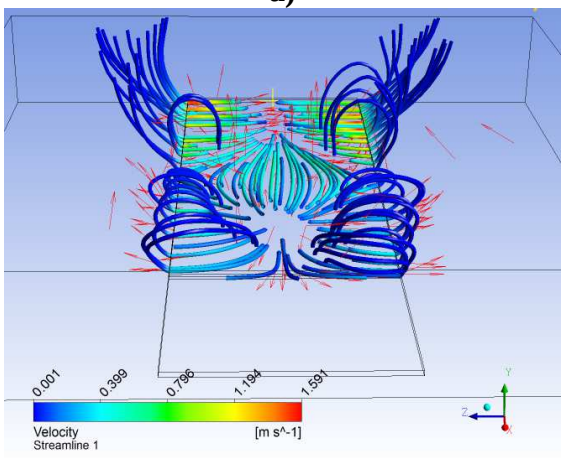

b)

Fig. 8. Streamlines spectrum. a) Time=36.5 μs; b) Time=109 μs.

From our preliminary studies on low density bridges, it seems that this feature is strongly associated with the high density of the bridge material (gold), which in turn, means that the inertial forces are responsible for this delay. Viscous damping acts as a high frequency cut-off filter, especially when the damping coefficient is rather low. The velocity field structure is represented in the figures below.

The streamlines depicted in Figs. 8a-b confirm not only the large pressure variation under the bridge but also the existence of two pressure extremes (a positive one and a negative one) that travels along the plate. Over the 200 μs duration, the relative pressure varies between +10000 Pa and -6500 Pa. This means that linearization of the Reynolds equations is no longer valid. On the other hand, along the edges of the bridge there is a strong fluid circulation which, for higher actuation frequency, may lead to detached vortices formation.

The step load case shows similar overall characteristics.

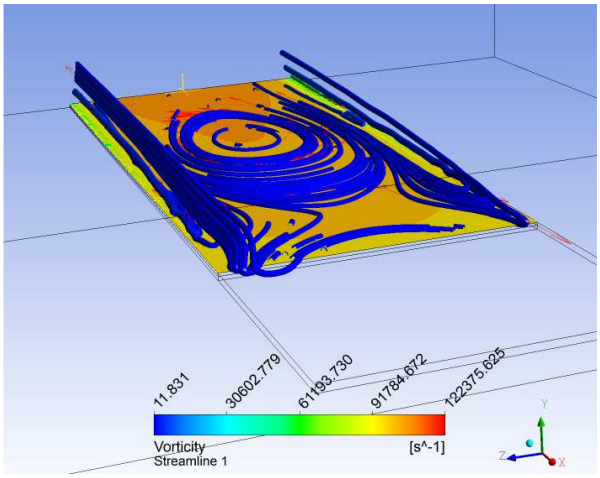

Fig. 9. Vortex lines and pressure distribution on the top side of the bridge (76.6 μs).

As expected, there is a consistent distribution of vortex lines that span the entire edges of the bridge (Fig. 9). These lines appear either detached or attached to the surface of the bridge. Concurrently, on top of the plate there is evidence of another major vortex structure.

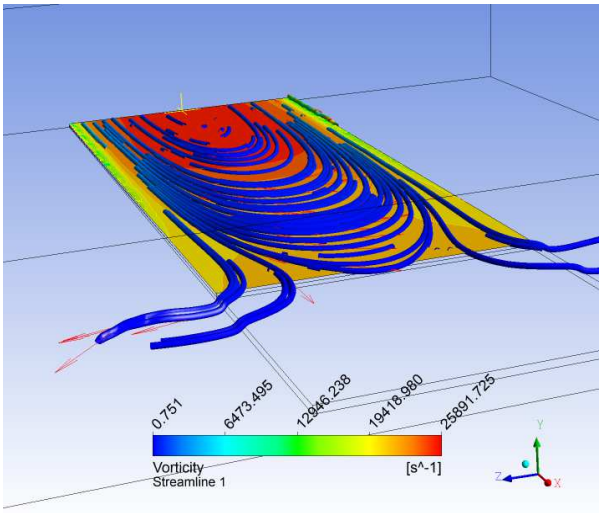

Fig. 10. Vortex lines and pressure distribution on the top side of the bridge (Time 255 μs).

The vortex eye illustrated in Fig. 9 is related to a pressure minimum on the fluid-solid interface. Most of the vortex spectrum is characterized by low frequencies of order tens of Hertz, but along the edges of the bridge close to the symmetry plane there are however vortices of tens of kHz magnitude. This large

spectrum of time scales is likely to affect the behaviour of the bridge for certain values of the actuation frequency.

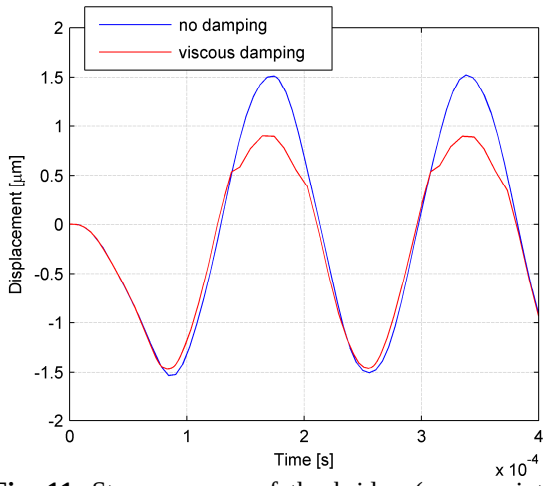

Fig. 11. Step response of the bridge (same point like previous).

The pressure distributions plotted in Figs. 9-10 shows that constant pressure paradigm on the top side of the plate is questionable. We acknowledge that pressure variation is however small in the order of tens of Pa.

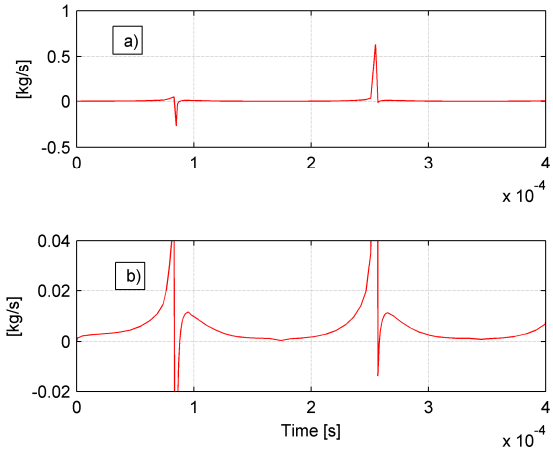

Fig. 12. Time variation of the damping coefficient; a) full view; b) detail view.

The temporal behaviour of the coefficient of damping associated with this actuation (Figs. 11-12) presents the same features like in the previous case. The negative values depicting a delay between the average velocity of the bridge and the aerodynamic force may lead to displacement amplifications in certain circumstances. It is not the case in our simulation due to high inertial forces that smooth out these very short negative peaks.

5. Conclusions

Our analysis showed that in cases when the relative pressure in the squeezed film becomes important the linearization of Reynolds equations fails. On the other hand, the top of the plate exhibits mild pressure variations and sustains consistent vortex structures with magnitudes in a very large spectrum. From this point of view, the smallest fluid dynamics temporal scale in the range of tens of kHz could be strongly coupled with the actuation frequency, hence yielding unpredictable behaviour of the structure.

The viscous damping coefficient is variable in time. The aerodynamic damping is most effective at high average velocities of the bridge. At the same time, higher oscillation modes are filtered-out through this damping mechanism.

Acknowledgement

This work has been funded by the Joint Research Project PN-II-PT-PCCA-2011-3, with the support of ANCS, CNDI – UEFISCDI, project no. 5/2012.

References

Andrews, M., I. Harris, I. and Turner, G., 1993. A comparison of squeeze-film theory with measurements on a microstructure, *Sens. Actuators A, Phys.*, vol. 36, no. 1, pp. 79–87.

Avdeev, I., 2003. New Formulation for Finite Element Modeling Electrostatically Driven Microelectromechanical Systems, PhD thesis, University of Pittsburg, United States of America.

Bao, M. and Yang, H., 2007. Squeeze film air damping in MEMS. *Sens. Actuators A* 136:3-27.

Eriksson, A., 2005. Mechanical Model of Electrostatically Actuated Shunt Switch, Excerpt from the Proceedings of the COMSOL Multiphysics User's Conference 2005 Stockholm.

Gyimesi, M and Ostergaard, D., 1999. Electro-

Mechanical Transducer for MEMS Analysis in ANSYS, in International Conference on Modeling and Simulation of Microsystems - MSM 1999, Puerto Rico, USA, NSTI.

Lee, K.B., 2011. Principles of Micro-electromechanical systems.

Mohite, S.S., Venkata R. S. and Rudra P., 2008. A Compact Squeeze-Film Model Including Inertia, Compressibility, and Rarefaction Effects for Perforated 3-D MEMS Structures, Journal of Microelectromechanical Systems, vol. 17, no. 3, pp. 709-723.

Steeneken, P.G., Rijks, Th.G.S.M., van Beek, J.T.M., Ulenaers, M.J.E., De Coster, J. and Puers, R., 2005. Dynamics and squeeze film gas damping of a capacitive RF MEMS switch, Journal of Micromechanics and Microengineering Volume 15 Number 1, pp.176.

Reza N.J., 2012. Nonlinear Modeling of Squeeze-Film Phenomena in Microbeam MEMS, in: L. Dai and R.N. Jazar (eds.), *Nonlinear Approaches in Engineering Applications*, Springer.

Veijola, T., 2001. Acoustic impedance elements modeling oscillating gas flow in micro channels, in *Proc. 4th Int. Conf. Model. Simul. Microsyst.*, Hilton Head Island, SC, pp. 96–99.

Veijola, T., 2004. Compact models for squeezed-film dampers with inertial and rarefied gas effects, *J. Micromech. Microeng.*, vol. 14, no. 7, pp. 1109–1118.

Veijola, T., 1999. Equivalent circuit model for micromechanical inertial sensors. Circuit Theory Laboratory Report Series CT-39, Helsinky University of Technology.